Effects of interfacial suboxides and dangling bonds on tunneling current through nanometer-thick SiO_2 layers

Eunjung Ko,[1,2] Kwang-Ryeol Lee,[3] and Hyoung Joon Choi[1,*]

[1]*Department of Physics and IPAP, Yonsei University, Seoul 120-749, Republic of Korea*

[2]*Center for Academic Computing, College of Applied Science, Kyung Hee University, Yongin 446-701, Republic of Korea*

[3]*Computational Science Center, Interdisciplinary Fusion Technology Division, KIST, Seoul 130-650, Republic of Korea*

(Received 29 October 2010; published 20 July 2011)

Quantum-mechanical tunneling of charge carriers through nanometer-thick SiO_2 layers is one of the key issues in Si-based electronics. Here, we report first-principles transport calculations of charge-carrier tunneling through nanometer-thick SiO_2 layers in $Si/SiO_2/Si$ structures. We find that tunneling of holes in the valence bands occurs mainly via oxygen $2p$ orbitals perpendicular to Si–O–Si bonds, and it can be enhanced greatly by interfacial suboxides and dangling bonds in Si/SiO_2 interfaces. Electrons in the conduction bands show tunneling behaviors sensitive to their wave vectors parallel to the interfaces, reflecting the six conduction-band minima in the bulk Si. Our results provide atomistic description of tunneling currents through SiO_2 layers, and suggest that leakage current will be blocked more effectively if suboxides and dangling bonds are reduced.

DOI: 10.1103/PhysRevB.84.033303 PACS number(s): 73.40.Gk, 71.15.Mb, 73.40.Ty, 85.30.De

SiO_2 is a key material in Si-based electronic devices, playing an important role of confining charge carriers within designed paths. However, in nanometer-scale devices where required SiO_2-layer thickness is 1 nm or less, it is highly challenging to enforce the role of SiO_2, since quantum-mechanical tunneling of charge carriers may contribute substantially to leakage current. Moreover, interfacial regions around SiO_2 layers become very significant when the layers have nanometer-scale thickness.

Atomic and electronic structures in Si/SiO_2 interfaces have been widely studied experimentally such as x-ray photoelectron spectroscopy,[1] electron energy loss spectroscopy,[2] core-level spectroscopy,[3] and Si $2p$ photoemission spectroscopy.[4] These experiments indicate, in common, that Si suboxide (SiO_x, $x < 2$) layers exist at the boundaries of SiO_2 layers, exhibiting all oxidation states. Since the energy gap in the suboxides is smaller than in SiO_2, their presence may weaken the current-blocking role of 1-nm-thick SiO_2 layers even further.[2,5]

Tunneling current through SiO_2 layers has been theoretically studied using continuum models based on effective-mass equations,[6–8] followed by atomic models using semiempirical tight-binding methods.[9] Since atomic and electronic structures at interfaces and defects become more important in nanometer-thick SiO_2 layers, first-principles calculations are needed to describe the tunneling current more accurately; however, such calculations[10,11] are still rarely reported.

In this Brief Report, we present first-principles density functional calculations of tunneling currents through SiO_2 layers in $Si(001)/SiO_2/Si(001)$ structures. We consider various SiO_2 thicknesses and different distributions of silicon suboxides, dangling bonds, and hydrogen atoms at interfaces. It is shown below that tunneling current is large if silicon suboxides distribute broadly or if the dangling bonds are present. Hole tunneling is found to occur dominantly via oxygen $2p$ orbitals perpendicular to Si–O–Si bonds and electron tunneling depends sensitively on wave vectors parallel to the interface, reflecting the presence of six conduction-band minima in bulk Si.

For simple atomic models for $Si(001)/SiO_2/Si(001)$ structures, we consider a slab of SiO_2 in the β-cristobalite structure with oxygen-terminated (001) surfaces on both sides. We place the slab between two Si(001) surfaces, expanding slightly the in-plane unit cell of SiO_2 on (001) surface to 0.7679×0.7679 nm^2 to match it with $\sqrt{2} \times \sqrt{2}$ supercell of Si on (001) surface. When the SiO_2 slab and two Si surfaces are just connected, half of Si atoms on each Si surface have dangling bonds due to the bond density mismatch. Depending on how to treat the dangling bonds, one has different interfacial structures. Here, we consider three types of Si/SiO_2 interfaces as shown in Fig. 1: (i) interfaces with suboxide transition layers (STLs), (ii) abrupt interfaces with dangling bonds (DBs), and (iii) abrupt interfaces with H atoms added to passivate dangling bonds (H-type).

In the STL-type interfaces [Figs. 1(a) and 1(b)], all dangling bonds are removed by rearranging oxygen atoms at the interfaces.[12] This oxygen rearrangement is equivalent to slight diffusion of oxygen atoms from SiO_2 to Si regions, broadening distributions of Si suboxides, so that Si atoms at the Si (001) surfaces have either Si^{1+} or Si^{2+} oxidation states ($Si^{1.5+}$ in average) while Si atoms at the first Si layers inside the SiO_2 region from either side are reduced from Si^{4+} to Si^{3+}. In DB-type interfaces [Fig. 1(c)], the SiO_2 slab and Si (001) surfaces are simply brought together and no treatment is done for the dangling bonds. Thus, half of Si atoms in the Si(001) surfaces are Si^{2+} while the other Si atoms have two dangling bonds. H-type interfaces [Fig. 1(d)] are the same as DB-type interfaces except that H atoms are introduced to passivate the dangling bonds. In DB- and H-type interfaces, Si^{4+} oxidation states in the SiO_2 region are not changed at all. Among the considered structures, the STL-type interfaces are most relevant in describing oxidized Si surfaces experimentally reported.[4]

In each $Si/SiO_2/Si$ structure, detailed atomic positions are obtained by relaxing the positions until all residual forces are smaller than 0.09 eV/Å, using the first-principles density functional method as implemented in SIESTA.[13] The supercell length in the ⟨001⟩ direction is also relaxed in each structure

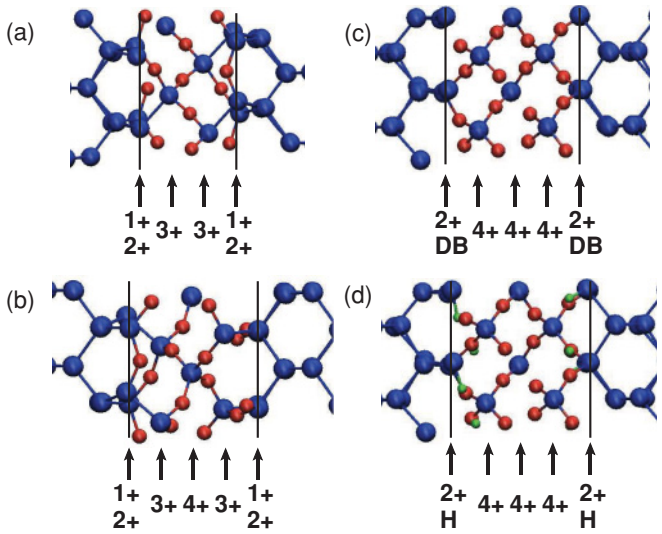

FIG. 1. (Color online) Atomic structures of $Si/SiO_2/Si$ structures (a) with suboxide transition layers (STLs) and SiO_2 thickness (d_{SiO_2}) of 0.54 nm, (b) with STLs and $d_{SiO_2} = 0.64$ nm, (c) with dangling bonds (DBs) and $d_{SiO_2} = 0.71$ nm, and (d) is the same as (c) except for additional H atoms passivating dangling bonds. Large (blue), small (red), and tiny (green) balls are Si, O, and H atoms, respectively. Si oxidation states, Si atoms with dangling bonds, and Si atoms bonding with H atoms are indicated with integer+, DB, and H, respectively. Vertical solid lines denote averaged Si positions on Si (001) surfaces, with which we measure d_{SiO_2}. In (d), only H atoms are relaxed after they are introduced in (c).

for minimal total energy. The local density approximation (LDA) is used for the exchange-correlation energy, and norm-conserving pseudopotentials[14] for electron-ion interactions. Real-space grids are generated with the cutoff energy of 200 Ry and pseudoatomic orbitals (double ζ polarization) are used to expand the electronic wave functions. For Brillouin-zone integration, a $4 \times 4 \times 4$ k-grid is used for the electron density during structure relaxation, and a 12×12 $k_\parallel$-grid for the tunneling current using the first-principles scattering-state method.[15] For Fig. 1(a), the resistive region and two intermediate regions in the scattering-state calculation contain 104 Si and 12 O atoms, and each unit cell of two Si bulk regions has 32 Si atoms.

In Fig. 1, SiO_2 thickness (d_{SiO_2}) is the distance between averaged Si positions on Si (001) surfaces marked with vertical lines. After full relaxation including the ⟨001⟩ length of the supercell, d_{SiO_2}'s in STL-type $Si/SiO_2/Si$ structures are ∼0.07 nm smaller than those in the DB- and H-type cases having the same number of O atoms. For comparison, we generate two types of H-type structures: one by relaxing only H atomic positions after H atoms are introduced to fully relaxed DB-type interfaces [Fig. 1(d)], and the other by relaxing all atoms.

In our calculations, band gaps of bulk Si and bulk SiO_2 are 0.54 and 6.73 eV, respectively, and they underestimate corresponding experimental values, 1.12 and 8.90 eV, which is a well-known feature of LDA results. Precise estimates of the energy gaps require methods beyond the density functional theory (DFT) such as GW methods.[16] For Si/SiO_2 interfaces, the experimental conduction band offset is 3.1 eV for $d_{SiO_2} \geqslant 1$ nm (Ref. 17) and the experimental valence band offset is 4.49 eV for $d_{SiO_2} \geqslant 1.6$nm.[18] For comparison, we determine band offsets in our $Si/SiO_2/Si$ structures by neglecting the projected density of states less than 0.01 states/eV inside SiO_2 layers. Our calculated conduction and valence band offsets are 2.58 and 2.47 eV, respectively, in the STL case with $d_{SiO_2} = 2.04$ nm, and 2.65 and 2.72 eV, respectively, for the H-type case with $d_{SiO_2} = 2.11$ nm. These results underestimate experimental values due to the LDA method, so our calculated tunneling current presented below may overestimate actual values in real samples; however, our results are still relevant as we compare effects of different interfacial structures.

Figure 2 shows the tunneling spectra $T(E)$ as a function of charge-carrier energy E for SiO_2 thickness ranging from 0.54 to 2.11 nm. The tunneling spectra $T(E)$ are the sum of $T_n(E)$ which is the tunneling probability of the nth channel averaged over wave vector $k_\parallel$ parallel to the interface. The spectra $T(E)$ are proportional to the cross-sectional area A of the interface in the supercell because the number of channels in the supercell is proportional to A. In our calculations, $A = 0.7679 \times 0.7679$ nm^2. In Fig. 2, all $T(E)$ are zero in the energy window from 0.0 to 0.54 eV due to the band gap in bulk Si. Overall SiO_2-thickness dependence shows that $T(E)$ drops by about 4 orders in magnitude as the SiO_2 thickness is increased from 0.64 to 1.34 nm in STL structures [Fig. 2(b)] and from 0.71 to 1.41 nm in DB- and H-type structures [Figs. 2(b) and 2(c)]. When the SiO_2 thickness is further increased from 1.34 to 2.04 nm in STL structures [Fig. 2(b)] and from 1.41 to 2.11 nm in DB- and H-type structures [Figs. 2(b) and 2(c)], $T(E)$ drops by about 3 and 2 orders in magnitude in the valence and conduction bands, respectively.

With STLs [Fig. 2(a)], $T(E)$ shows rather monotonous exponential dependence on the energy E within 1 eV near the band gap. In comparison, dangling bonds [Fig. 2(b)] greatly enhance $T(E)$ near the valence band maximum (VBM), with substantial increase in $T(E)$ near the conduction band minimum (CBM). In contrast, H atoms passivating the dangling bonds [Fig. 2(c)] make $T(E)$ near VBM even smaller

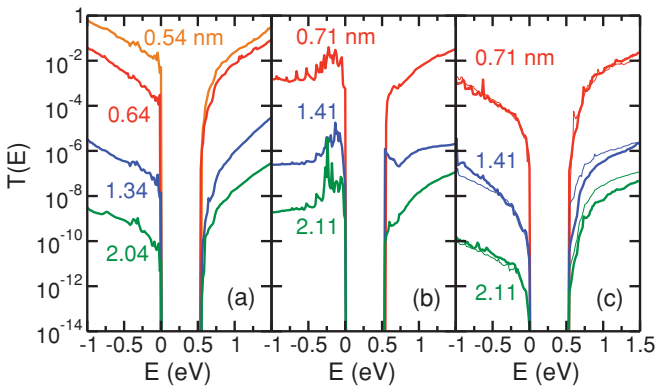

FIG. 2. (Color online) Tunneling spectra, $T(E)$, vs energy, E, in $Si/SiO_2/Si$ structures with (a) the STL-, (b) DB-, and (c) H-type Si/SiO_2 interfaces. The tunneling spectra are obtained by average over a 12×12 $k_\parallel$-grid. The valence band maximum is set to be zero. Thicknesses of SiO_2 layers in nm are given inside the plots. In (c), thick and thin lines are for H-only and all-atom relaxed cases, respectively.

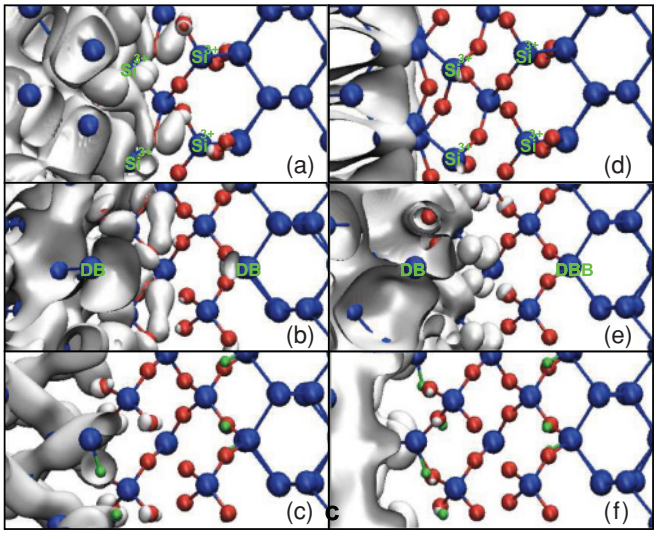

FIG. 3. (Color online) Isosurface plots of scattering-state wave functions for maximally tunneling eigenchannels at $\mathbf{k}_\parallel = 0$ incident from the left. (a)–(c) are at the valence band maximum and (d)–(f) are at the conduction band minimum of Si regions. (a) and (d) are for the STL-type interface [Fig. 1(b)], (b) and (e) are for the DB-type [Fig. 1(c)], and (c) and (f) are for the H-only relaxed H-type [Fig. 1(d)]. Large (blue), small (red), and tiny (green) balls are Si, O, and H atoms, respectively.

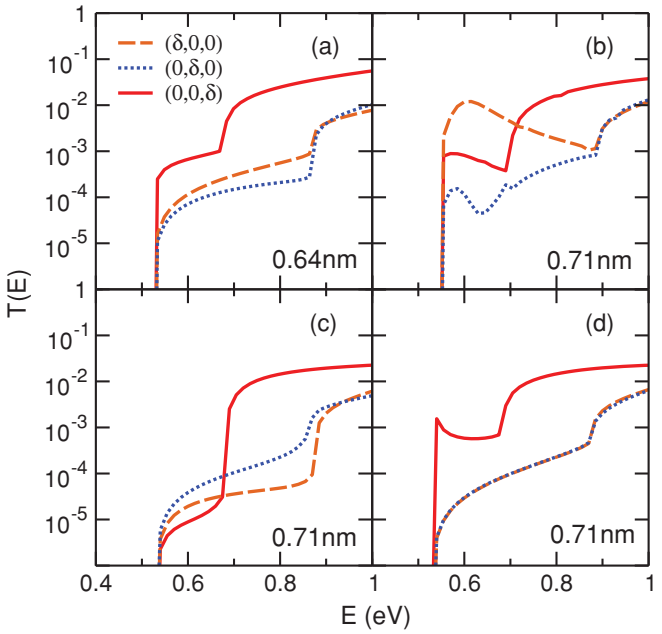

FIG. 4. (Color online) $\mathbf{k}_\parallel$-dependent tunneling spectra, $T(E,k_\parallel)$, near the conduction band minima for different interfaces: (a) the STL-type [Fig. 1(b)], (b) the DB-type [Fig. 1(c)], (c) the H-only relaxed H-type [Fig. 1(d)], and (d) the all-atom relaxed H-type interface. In (a)–(d), tunneling spectra for $\mathbf{k}_\parallel$ corresponding to the conduction band minima at $(\delta,0,0)$, $(0,\delta,0)$, and $(0,0,\delta)$ of bulk Si are represented with dashed (orange), dotted (blue), and solid (red) lines, respectively. The valence-band maximum is set to zero in energy.

than those in STL-type cases. We also note in Fig. 2(c) that $T(E)$ is slightly different for two different H-type structures: one from relaxing H atoms only and the other from relaxing all atoms.

To find out major tunneling path of electrons and holes through the barriers, we performed eigenchannel analysis and obtained scattering-state wave functions of the maximally tunneling eigenchannels near VBM and CBM at $\mathbf{k}_\parallel = 0$ (Fig. 3). Our eigenchannel analysis shows that only one eigenchannel (or rarely two) dominates the tunneling near VBM. With STLs, Si^{1+}–Si^{3+} bonds are important paths through which the hole tunneling occurs [Fig. 3(a)]. While dangling bonds enhance the hole tunneling greatly [Fig. 3(b)], H atoms passivating the dangling bonds suppress the tunneling [Fig. 3(c)]. Inside SiO_2 region, the hole tunneling occurs dominantly through O $2p$ orbitals perpendicular to Si–O–Si bonds. This reflects that states near VBM in bulk SiO_2 are mainly from O $2p$ orbitals perpendicular to the bonds,[19] which is correctly described by the DFT as well as GW methods.[16]

Interfacial atomic structures have comparatively weak, but still significant, influence on maximally tunneling eigenchannels near CBM at $\mathbf{k}_\parallel = 0$, as shown in Figs. 3(d)–3(f). Si $3s$ and O $3s$ orbitals, which are important in states near CBM in bulk SiO_2,[19] are affected by the suboxide states and the H atoms, and dangling-bond states near CBM have significant influences on tunneling eigenchannels.

Figure 4 shows tunneling spectra $T(E,\mathbf{k}_\parallel)$ for different $\mathbf{k}_\parallel$s corresponding to different bulk-Si CBMs. Let the six CBM of bulk Si be at, say, $\mathbf{k} = (\pm\delta,0,0)$, $(0,\pm\delta,0)$, and $(0,0,\pm\delta)$. Since the tunneling direction is along $\langle 001\rangle$ in our systems, two CBM at $\mathbf{k} = (0,0,\pm\delta)$ are mapped to $\mathbf{k}_\parallel = 0$ while the other four CBM are mapped to nonzero $\mathbf{k}_\parallel$s. With suboxide layers [Fig. 4(a)], $T(E,\mathbf{k}_\parallel)$ is the largest near $\mathbf{k} = (0,0,\delta)$ in the energy range from 0.54 to 0.64 eV, while dangling bonds [Fig. 4(b)] make the tunneling near $\mathbf{k} = (\delta,0,0)$ be the largest. When the dangling bonds are passivated by H atoms, the tunneling is the largest near $\mathbf{k} = (0,\delta,0)$ in the H-only relaxed case [Fig. 4(c)], but it is the largest near $\mathbf{k} = (0,0,\delta)$ in the all-atom relaxed case [Fig. 4(d)]. Thus, contributions

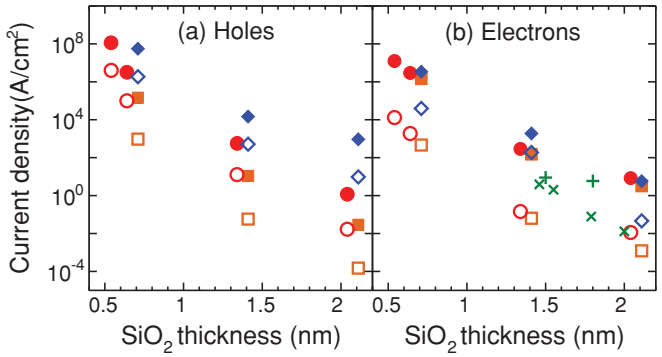

FIG. 5. (Color online) Tunneling current density of (a) holes and (b) electrons vs SiO_2 thickness, obtained by Eqs. (1) and (2), respectively. Open and solid symbols are for carrier concentrations of 1×10^{18} cm^{-3} and 1×10^{20} cm^{-3}, respectively, (red) circles are for the interfaces with STLs, (blue) diamonds are with DBs, and (orange) squares are with H atoms passivating DBs (only H atoms relaxed). In (b), plus (+) and cross (×) symbols, drawn for comparison, indicate measured values of leakage current at the gate voltage of 1 V in Refs. 20 and 21, respectively.

of different conduction band minima to $T(E)$ are sensitive to interfacial atomic structures.

We consider the tunneling current density per unit area through a SiO_2 layer when the two Si regions have different chemical potentials which make one of the two Si regions has a substantial concentration of electrons (n_e) or holes (n_h) while the other Si region has negligible carrier densities. Using $T(E)$ shown in Fig. 2, the tunneling current density J_h of holes in the valence bands is

$$J_h = \frac{1}{A}\frac{2e}{h}\int_{-\infty}^{\mathrm{VBM}} T(E)(1 - f(E))dE, \quad (1)$$

and the tunneling current density J_e of electrons in the conduction bands is

$$J_e = \frac{1}{A}\frac{2e}{h}\int_{\mathrm{CBM}}^{\infty} T(E)f(E)dE, \quad (2)$$

where $f(E)$ is Fermi-Dirac distribution function at 300 K in the Si region in which n_e or n_h is substantial. Here, we neglect any effect of the nonzero charge-carrier concentration or nonzero finite bias on $T(E)$, so Eqs. (1) and (2) are accurate in the limit that the concentration is small. We calculate J_e and J_h for two different concentrations: 1×10^{18} cm^{-3} and 1×10^{20} cm^{-3} (Fig. 5). Corresponding chemical potentials are located at 0.01 eV below CBM for $n_e = 1 \times 10^{18}$ cm^{-3}, 0.31 eV above CBM for $n_e = 1 \times 10^{20}$ cm^{-3}, 0.02 eV below VBM for $n_h = 1 \times 10^{18}$ cm^{-3}, and 0.35 eV below VBM for $n_h = 1 \times 10^{20}$ cm^{-3}, which are determined from the density of states in bulk Si. As shown in Fig. 5(b), calculated J_e agrees with available experimental values[20,21] in the order of magnitude. Calculated tunneling currents for the H-type cases are slightly smaller than for the STL-type and substantially smaller than for the DB-type, showing again that STLs and dangling bonds enhance tunneling current, respectively.

In summary, we presented tunneling properties of SiO_2 layers in Si(001)/SiO_2/Si(001) structures with SiO_2 thickness from 0.54 to 2.11 nm by using a first-principles scattering-states method. Our results show that interfacial suboxides and dangling bonds enhance the tunneling greatly, so the abrupt interfaces with no suboxides and no dangling bonds can reduce the tunneling currents. Eigenchannel analysis showed that the major tunneling paths near VBM are O p orbitals perpendicular to Si–O–Si bonds. Tunneling near CBM depends sensitively on the wave vector parallel to the interface, reflecting the presence of multiple CBM in bulk Si.

This work was supported by NRF of Korea (Grant No. 2009-0081204) and by the Converging Research Center Program through the Ministry of Education, Science and Technology (2010K000992). Computational resources have been provided by KISTI Supercomputing Center (Project No. KSC-2008-S02-0004).

*h.j.choi@yonsei.ac.kr

[1] F. J. Grunthaner, P. J. Grunthaner, R. P. Vasquez, B. F. Lewis, J. Maserjian, and A. Madhukar, J. Vac. Sci. Technol. **16**, 1443 (1979); A. Ishizaka and S. Iwata, Appl. Phys. Lett. **36**, 71 (1980).

[2] D. A. Muller, T. Sorsch, S. Moccio, F. H. Baumann, K. Evans-Lutterodt, and G. Timp, Nature **399**, 758 (1999).

[3] G. Hollinger and F. J. Himpsel, Appl. Phys. Lett. **44**, 93 (1984); F. J. Himpsel, F. R. McFeely, A. Taleb-Ibrahimi, J. A. Yarmoff, and G. Hollinger, Phys. Rev. B **38**, 6084 (1988).

[4] K. Ohishi and T. Hattori, Jpn. J. Appl. Phys. **33**, L675 (1994); J. H. Oh, H. W. Yeom, Y. Hagimoto, K. Ono, M. Oshima, N. Hirashita, M. Nywa, A. Toriumi, and A. Kakizaki, Phys. Rev. B **63**, 205310 (2001).

[5] M. Schulz, Nature **399**, 729 (1999); D. A. Muller, Nat. Mater. **4**, 645 (2005).

[6] H. Nakatsuji and Y. Omura, Jpn. J. Appl. Phys. **39**, 424 (2000).

[7] M. Fukuda, W. Mizubayashi, A. Kohno, S. Miyazaki, and M. Hirose, Jpn. J. Appl. Phys. **37**, L1534 (1998).

[8] Khairurrijal, W. Mizubayashi, S. Miyazaki, and M. Hirose, Appl. Phys. Lett. **77**, 3580 (2000).

[9] M. Städele, B. R. Tuttle, and K. Hess, J. Appl. Phys. **89**, 348 (2001).

[10] A. A. Demkov, X. Zhang, and D. A. Drabold, Phys. Rev. B **64**, 125306 (2001); X.-G. Zhang, Z.-Y. Lu, and S. T. Pantelides, Appl. Phys. Lett. **89**, 032112 (2006).

[11] J. Kang, Y.-H. Kim, J. Bang, and K. J. Chang, Phys. Rev. B **77**, 195321 (2008); T. Ono, *ibid.* **79**, 195326 (2009).

[12] I. Ohdomari, H. Akatsu, Y. Yamakoshi, and K. Kishimoto, Non-Cryst. Solids **89**, 239 (1987); J. Appl. Phys. **62**, 3751 (1987).

[13] D. Sánchez-Portal, P. Ordejón, E. Artacho, and J. M. Soler, Int. J. Quantum Chem. **65**, 453 (1997).

[14] N. Troullier and J. L. Martins, Phys. Rev. B **43**, 1993 (1991).

[15] H. J. Choi, M. L. Cohen, and S. G. Louie, Phys. Rev. B **76**, 155420 (2007).

[16] L. E. Ramos, J. Furthmüller, and F. Bechstedt, Phys. Rev. B **69**, 085102 (2004).

[17] V. V. Afanas'ev, M. Houssa, A. Stesmans, and M. M. Heyns, Appl. Phys. Lett. **78**, 3073 (2001).

[18] J. L. Alay and M. Hirose, J. Appl. Phys. **81**, 1606 (1997).

[19] P. M. Schneider and W. B. Fowler, Phys. Rev. Lett. **36**, 425 (1976).

[20] H. S. Momose *et al.*, IEEE Trans. Electron Devices **43**, 1233 (1996).

[21] N. Yang, W. K. Henson, J. R. Hauser, and J. J. Wortman, IEEE Trans. Electron Devices **46**, 1464 (1999).